Hot Corrosion Resistance of Aluminosilicate Refractories – Comparative Tests in the Secondary Combustion Chamber of a Hazardous Waste Incinerator

A. Villalba Weinberg, C. Varona, X. Chaucherie, J. Poirier, D. Goeuriot

Dedicated to the 10th Anniversary of refractories WORLDFORUM

This paper presents the alkali and sulphur vapour corrosion resistance of aluminosilicate refractories under industrial conditions. Aluminosilicate refractory samples with Al_2O_3 contents ranging 42–90 mass-% were exposed for 8 months to the corrosive atmosphere in the secondary combustion chamber (gas temperature approx. 950 °C) of a hazardous waste incineration facility. After the exposure, the samples were analysed in the laboratory regarding porosity and mineralogical changes.

The test results show that degradation is caused by hot corrosion, specifically by condensed thenardite (Na_2SO_4). Free silica, largely accessible in fireclay bricks, is the first phase that reacts with thenardite. The reaction generates liquid natrosilite ($Na_2Si_2O_5$). This low melting phase leads to deformation and creep of hotter brick parts. In a next step, natrosilite reacts with mullite forming albite ($NaAlSi_3O_8$). Simultaneously, thenardite reacts directly with mullite forming nosean ($Na_8Al_6Si_6O_{28}S$).

In order to better withstand the hot corrosion mechanism, refractories should contain as little silica as possible.

1 Introduction

Alkali attack is an important problem that refractories have to encounter in many applications. The thermodynamic stability of the refractory in contact with the alkalis depends on the brick temperature and the chemical and mineralogical composition of the refractory. In the literature, exhaustive studies by Jacobson et al. on Al_2O_3–SiO_2 ceramics indicate that at temperatures below 1100 °C [1–5], high alumina contents are more resistant, whereas at temperatures above 1100 °C, low alumina contents should be preferred in view of the detrimental β-alumina formation. Under industrial conditions, this empirical rule of thumb needs to be confirmed by tests before choosing a refractory material. The present study deals with the interactions between aluminosilicate refractories and the corrosive environment in the secondary combustion chamber of a hazardous waste incinerator.

The function of the secondary combustion chamber is to destroy toxic organic gases at a consistently high temperature (>850 °C) for at least 2 s. The temperature is kept in the present study at 930–1000 °C via a gas burner. However, in other plants, the temperature can be even higher (1100–1150 °C), depending on the chlorine content in the waste. The secondary combustion chamber studied here was double lined with two bricks of 220 mm thickness and a supplemental layer of insulating refractory bricks to reduce heat losses (Fig. 1). Consequently, the thermal gradient in the working lining is not elevated, and temperatures of the cold side of the working lining remain rather high, at approximately 750 °C.

Gas and fly ash that leave the rotary kiln enter the chamber at the lower part and

Adrian Villalba Weinberg, Cyrille Varona
BONY SA – Produits Réfractaires
42001 Saint-Étienne
France

Xavier Chaucherie
SARPI-VEOLIA
78520 Limay
France

Jacques Poirier
CEMHTI CNRS UPR 3079
Université d'Orléans
45071 Orléans
France

Dominique Goeuriot
LGF CNRS UMR 5307, MINES Saint-Étienne
42023 Saint-Étienne
France

Corresponding author:
Adrian Villalba Weinberg
E-mail: a.villalba-weinberg@bony-sa.fr

Keywords: alkali attack, sulphur, mullite, hazardous waste incinerator

Received: 15.01.2018
Accepted: 21.01.2018
The paper received the 2nd Prize of the Poster Award launched by refractories WORLDFORUM at ICR™ 2017 in Aachen/DE

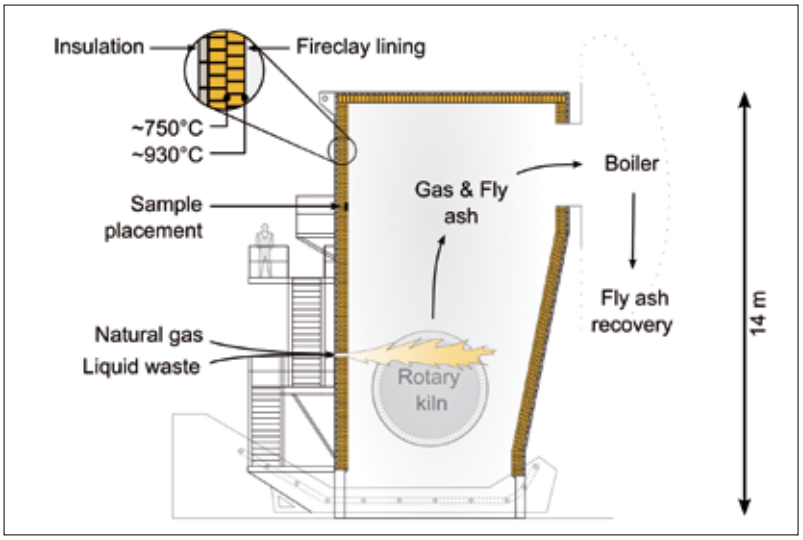

Fig. 1 Schematic draw of the secondary combustion chamber that served for the industrial test

rise to the outlet at the upper part of the chamber, where they enter the boiler. Low calorific liquid waste that cannot be treated in the rotary kiln is injected directly into the secondary combustion chamber through a nozzle located in the chamber wall next to the gas burner. Both natural gas and liquid waste can present challenging problems. One of the principal corrosive agents, sulphur, results from the combustion of natural gas or waste fuels that contain sulphur as an impurity [2, 3]. Added to that, the injected liquids are typically low calorific salty solutions that contain large amounts of destructive alkalis (mainly sodium and potassium). As the authors have shown in a previous paper [6], thermodynamic calculations indicate NaCl (g), KCl (g), NaF (g) and KF (g) to be the predominant alkali gases in the chamber and in the interior of the lining, which result from gas reactions between monoatomic Na (g), K (g) and HCl (g) and HF (g). The gaseous salts represent together with SO_2 (g) and SO_3 (g) the main corrosive agents. When cooling down, these corrosive vapours condense. Fly ash, recovered from the boiler, contains a significant portion of condensed matter that was in the gaseous state when it was flowing through the secondary combustion chamber. The overall fly ash composition is indicated in Tab. 1. Remarkable are the high amounts of Na_2O, SO_3, and Cl, which are notorious for being corrosive to refractories.

Widely used liner materials for this application are fireclay and high-alumina bricks with 40–60 mass-% Al_2O_3. Although the refractory lifetime of at least 5 years is rather satisfying, the problem of these materials is the unpredictability of failure. Some operators have reported sudden breakdowns of refractory walls that were visually intact.

The objectives of the present study were to find corrosion resistant and save refractory alternatives. For this purpose, state-of-the-art materials and alternative materials were tested for 8 months in the secondary combustion chamber of an industrial hazardous waste incinerator of SARPI-VEOLIA/FR and the corrosion resistance was evaluated afterwards.

Tab. 1 Typical fly ash composition [mass-%] recovered from the boiler; results obtained via X-ray fluorescence, except for sulphur, which was analysed using a combustion/absorption infrared spectroscopy

SiO_2	P_2O_5	Na_2O	K_2O	CaO	Fe_2O_3	F	Cl	SO_3
2,9	1,5	30,5	7,2	6,4	3,2	2,0	28,9	11,7

Tab. 2 Characteristics of the refractory materials tested in the secondary combustion chamber

Refractory	Fireclay	Andalusite	Bauxite, Clay	Corundum
Principal raw materials	Chamotte, clay	Andalusite, clay, phosphate	Bauxite, clay	Brown fused alumina, phosphate
Mineral phases	Mullite, amorphous phase, cristobalite	Mullite, andalusite, $AlPO_4$, amorphous phase	Mullite, corundum, amorphous phase	Corundum, mullite, $AlPO_4$
Composition [mass-%]				
Al_2O_3	42	60	67	90
SiO_2	52	37	29	6
Fe_2O_3	1,9	1,1	1,4	0,2
TiO_2	1,5	0,9	2,4	2,5
P_2O_5	–	1,5	–	1,5
CaO+MgO	1,1	0,2	0,1	0,3
Na_2O+K_2O	1,5	0,3	0,3	0,3
Open porosity [%]	16,0	11,8	24,8	14,1

2 Experimental

2.1 Materials tested

The materials tested were commercial fireclay and high-alumina refractory bricks. The composition and characteristics are summarized in Tab. 2. The fireclay and the bauxite-clay bricks are reference materials widely used as secondary combustion chamber liner materials. The andalusite and corundum bricks, both produced by BONY SA, were tested as potential alternatives.

Not only differs the Al_2O_3/SiO_2 among the tested materials, but also the porosity. This allows to examine the influence of both chemistry and porosity on the vapour corrosion resistance. The material with the highest porosity is the bauxite-clay brick. Its porosity of almost 25 % is due to the porous

bauxite aggregates used for the fabrication of this material.

2.2 Industrial test

The refractory samples were exposed for 8 months to the corrosive atmosphere in the secondary combustion chamber. The samples with dimensions 50 mm × 50 mm × 100 mm were placed in the refractory lining of a furnace door, located in the chamber sidewall above the burner (c.f. Fig. 1).

The samples' hot faces stood in contact with the harsh atmosphere of the secondary combustion chamber and the cold faces were in contact with the second working lining. No mortar was used in the joints between the samples.

2.3. Characterization

After the exposure, the samples were measured, cut, and analysed regarding porosity and mineralogical composition. A 10 mm slice was removed from the middle of each sample using a water-cooled diamond saw. Then, cut slices were photographed and measured.

X-ray diffraction (XRD) was conducted on 5 mm × 5 mm × 10 mm samples before and after the test to reveal possible phase transformations. These measurements were conducted at the "hot" face at 17 mm distance from the hot facing surface and at the cold face at 77 mm distance from the hot facing surface. No water was used for this cutting procedure to keep the dilution of salty phases to a minimum. The samples were ground to powder in a planetary ball mill (Pulverisette, Fritsch/DE), of which the recipient and the grinding balls were made of tungsten carbide. The powder was analysed with a Bragg-Brentano diffractometer (D8 Advance, Bruker/DE) using Cu K_α radiation.

Open porosity was measured via Archimedes' method on 5 mm × 5 mm × 10 mm samples at different brick regions (Fig. 2), according to DIN EN 993-1 [7]. Oil was used for the soaking step to prevent the possible dilution of salts.

3 Results and discussion

3.1 Macroscopic changes

After the 8 months exposure, the corrosive atmosphere has visually interacted with the refractory samples, as Fig. 3 manifests. Condensed matter and fly ash have deposited and stuck to the hot face, forming a thin corrosive deposit, which is rich in SiO_2, Na_2O, CaO, Fe_2O_3, and SO_3. The colour changes suggest that the hot facing side has been more corroded than the cold facing side.

Significant changes in size could not be observed, except for the fireclay brick, which expanded by 3,5 % in length. For the other materials, the 8 months testing period was too short to produce measurable swelling phenomena. Sections of the interior of the samples (Fig. 4) show that

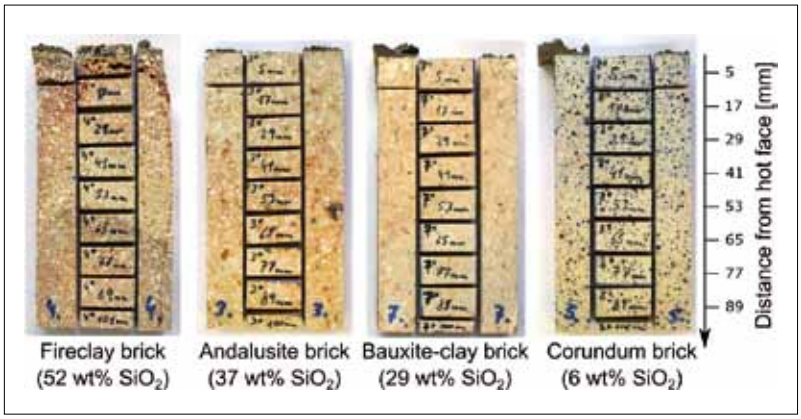

Fig. 2 Sampling for porosity and XRD measurements

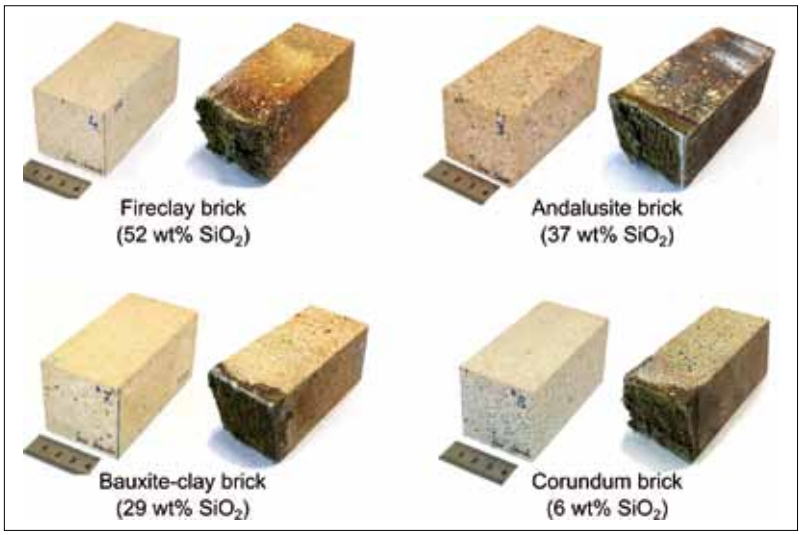

Fig. 3 Samples with dimensions (50 mm × 50 mm × 100 mm) before and after the test

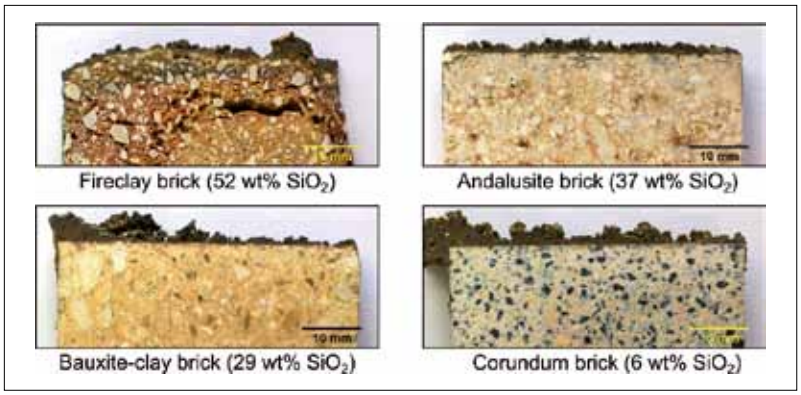

Fig. 4 Photographs of the transversally cut samples after an 8 months testing period in the secondary combustion chamber

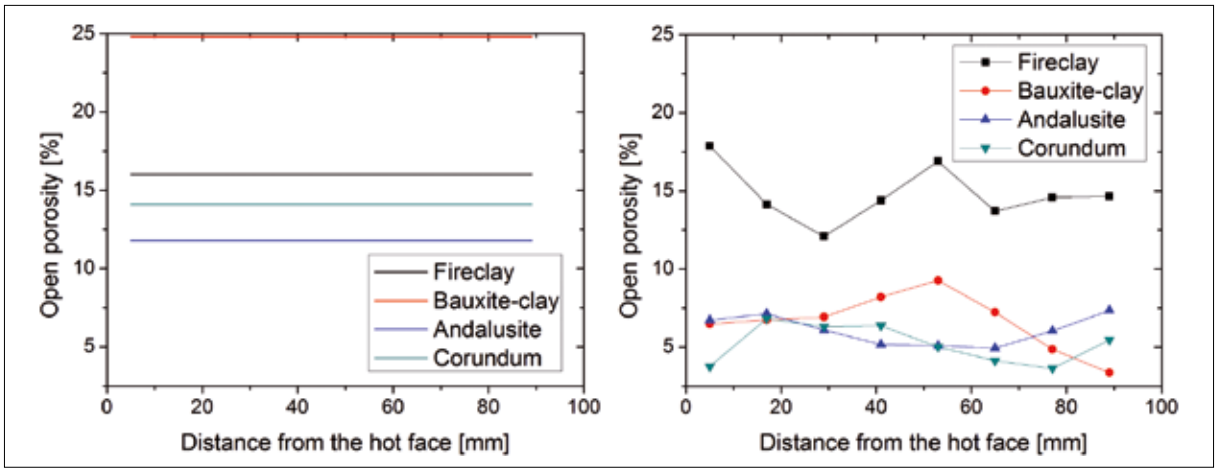

Fig. 5 Open porosity of the as-fabricated refractory products and after the 8 months exposure to the harsh atmosphere of the secondary combustion chamber

the corundum brick (6 mass-% SiO_2) has a clear-cut interface between the brick's hot face and the deposit. Visually, this brick seems unaffected. The bauxite-clay reference brick (29 mass-% SiO_2) appears to be little affected, as well. In the andalusite brick (36 mass-% SiO_2), small cracks are visible growing parallel to the hot face. The most degraded brick is the fireclay reference material, which is the sample with the highest silica content (52 mass-% SiO_2).

3.2 Porosity changes

Compared to the initial values of the materials as-fabricated, the test has drastically reduced the porosity (Fig. 5). In all bricks, the final porosity is at approximately 5 %, except for the fireclay sample, which is at 15 %.

The higher porosity in the fireclay brick could be explained by the volume expansion and the generated cracks that can be observed on the photograph.

Additionally, some natrosilite ($Na_2Si_2O_5$) may have dissolved into the water during the cutting procedure, seeing that natrosilite is a water-soluble corrosion product [3]. The most remarkable porosity change is measured in the bauxite-clay brick, where the porosity dropped by approx 20 %.

Note that the porosity has been closed even at the cold face of the samples, which means that the gas penetrated the bricks until the cold side and condensed over the entire length of the samples, regardless of the initial porosities of the as-fabricated materials.

3.3 Mineralogical changes

As to the mineralogical changes, notable amounts of amorphous phase have been formed during the test, which is reflected on the diffractogrammes by a hump at angles <15° (Fig. 6). The height of this hump correlates with the silica content: the higher the silica content, the more distinctive the hump appears. This indicates the dissolution of free crystalline silica in form of cristobalite or quartz and the formation of an amorphous, silica-rich phase. New crystalline phases are albite ($NaAlSi_3O_8$), nosean ($Na_8Al_6Si_6O_{28}S$), and thenardite (Na_2SO_4).

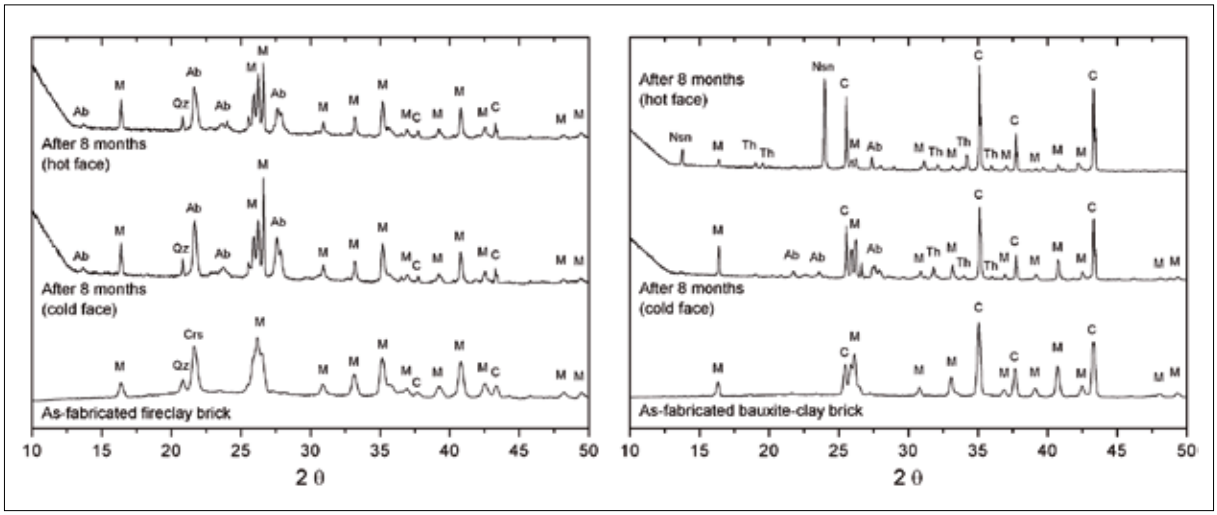

Fig. 6 X-ray diffraction patterns of the fireclay sample (52 mass-% SiO_2) and the bauxite-clay sample (29 mass-% SiO_2) before and after the test period of 8 months; mineralogical phases are C – corundum (Al_2O_3), M – mullite ($Al_6Si_2O_{13}$), Crs – cristobalite (SiO_2), Qz – quartz (SiO_2), Nsn – nosean ($Na_8Al_6Si_6O_{28}S$), Ab – albite ($NaAlSi_3O_8$), and Th – thenardite (Na_2SO_4)

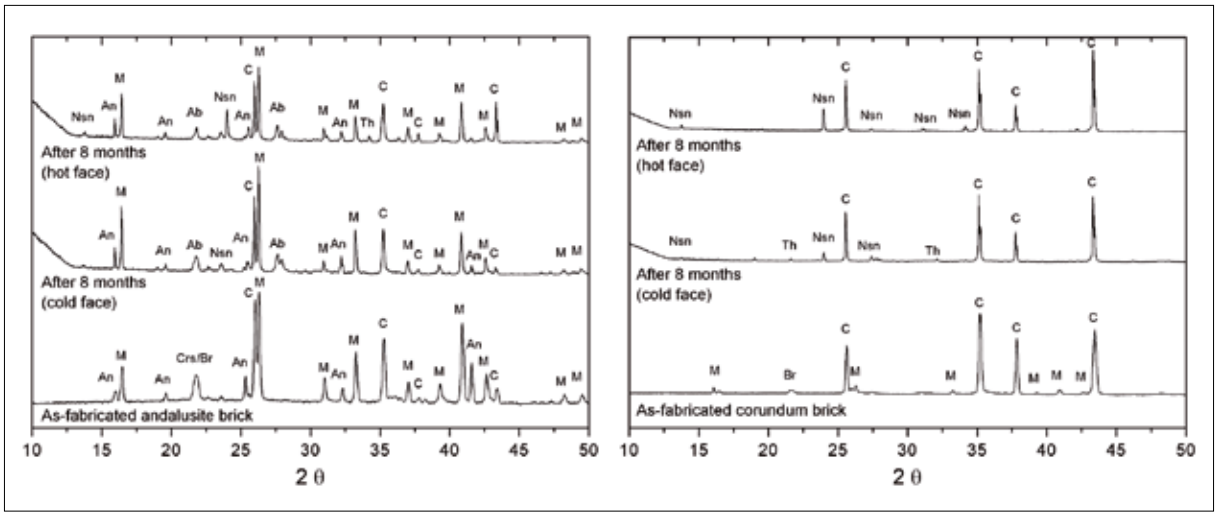

Fig. 7 X-ray diffraction patterns of the andalusite sample (37 mass-% SiO_2) and the corundum sample (6 mass-% SiO_2) before and after the test period of 8 months; mineralogical phases are C–corundum (Al_2O_3), M–mullite ($Al_6Si_2O_{13}$), An–andalusite (Al_2SiO_5), Br–berlinite ($AlPO_4$), Crs–cristobalite (SiO_2), Ab–albite ($NaAlSi_3O_8$), Nsn–nosean ($Na_8Al_6Si_6O_{28}S$), and Th–thenardite (Na_2SO_4)

Of note, free silica reacted almost completely after only 8 months in the chamber. On the other hand, mullite has been "consumed" only partially, except in the corundum bricks.

It can be therefore concluded that the corundum brick will not react further, as in this material thenardite finds no more mullite to react with. In contrast, for the samples other than the corundum brick, the corrosion process is not completed, yet.

These test results prove that the poorer the material in silica is, the better it resists to hot corrosion. The chemical stability of the phases increase in the following order: amorphous silica (SiO_2) < cristobalite (SiO_2) < quartz (SiO_2) < andalusite (Al_2SiO_5) < mullite ($Al_6Si_2O_{13}$) < corundum (Al_2O_3). Corundum is practically immune to alkali and sulphur at the present temperatures (<1100 °C).

3.4 Wear mechanism: hot corrosion

In all the analysed samples, new sodium and sulphur compounds have been identified. Both elements have penetrated the brick as gaseous compounds NaCl (g), NaF (g), SO_2 (g) and SO_3 (g), as we pointed out in more detail in [6].

Thanks to various exhaustive studies on combustion atmospheres at 700–1000 °C [1–3, 8–12], it is well known that, under these circumstances, thenardite (Na_2SO_4) likely condenses at colder parts of the furnace, which is in our case the refractory material. The technical term for corrosion by Na_2SO_4 is hot corrosion [5, 13]. The formation of Na_2SO_4 results from the reactions between gaseous salts, sulphur oxides, oxygen, and water vapour, as described by reaction (1).

$$2\ NaCl\ (g) + SO_2\ (g) + ½\ O_2 + H_2O\ (g) \rightarrow Na_2SO_4\ (s, l) + 2\ HCl\ (g) \quad (1)$$

Amorphous silica is the first "victim" of thenardite, followed by crystalline silica in the form of cristobalite, tridymite or quartz, which is attacked next.

It is important to note that liquid thenardite (T_m = 884 °C, [5]) reacts quicker with silica than in the solid state, due to higher diffusion rates. This explains why the hot face of the sample (at 930 °C) is more corroded than the colder side (at approx 800 °C). Reaction (2) is the most relevant reaction for the dissolution of free silica.

$$Na_2SO_4\ (l) + 2\ SiO_2\ (s) \rightarrow Na_2Si_2O_5\ (l) + SO_2\ (g) + ½\ O_2\ (g) \quad (2)$$

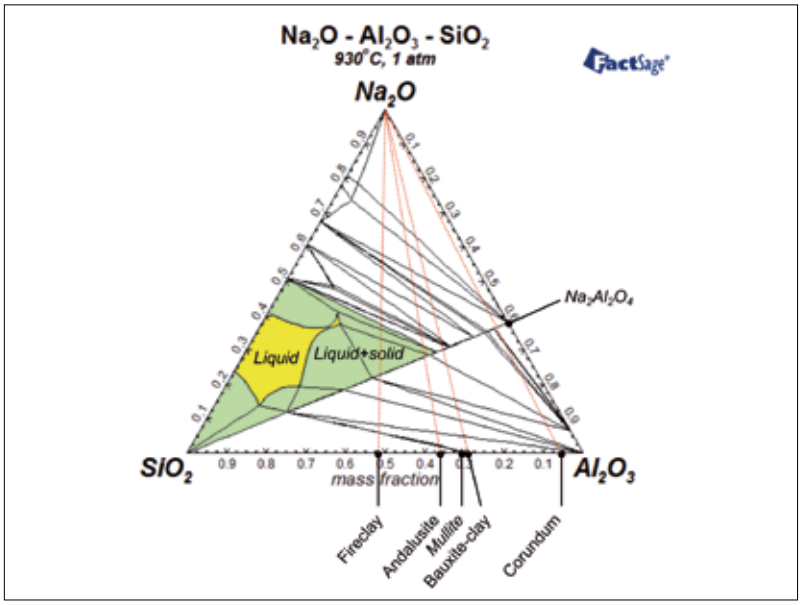

Fig. 8 Face diagram Na_2O–Al_2O_3–SiO_2 at 930 °C (hot face temperature), calculated using FactSage® 6.4

This reaction indicates that thenardite acts as a fluxing agent, dissolving free silica into the liquid. Molten thenardite combined with low melting natrosilite ($Na_2Si_2O_5$, T_m = 775 °C, [14]) forms copious amounts of liquid. The higher the silica content of the brick, the more liquid phase will form, as the phase diagram in Fig. 8 illustrates. Excessive amounts of liquid phase cause brick deformation and loss of mechanical strength and creep resistance. Therefore, the presence of free silica in the brick implies a higher risk of failure.

Once the free silica has been consumed, mullite ($Al_6Si_2O_{13}$) comes under attack. Liquid natrosilite ($Na_2Si_2O_5$) that was formed in the previous step reacts with mullite ($Al_6Si_2O_{13}$) to form albite ($NaAlSi_3O_8$) and alumina (reaction (3)).

$$Na_2Si_2O_5\ (l) + 2\ Al_6Si_2O_{13}\ (s) \rightarrow 2\ NaAlSi_3O_8\ (s) + 5\ Al_2O_3\ (s) \quad (3)$$

Simultaneously, Na_2SO_4 may react directly with mullite resulting in nosean. This corrosion step could be represented by reaction (4).

$$4\ Na_2SO_4\ (l) + 3\ Al_6Si_2O_{13}\ (s) \rightarrow Na_8Al_6Si_6O_{28}S\ (s) + 6\ Al_2O_3\ (s) + 3\ SO_2\ (g) + {}^3/_2\ O_2\ (g) \quad (4)$$

The crystal structure of nosean corresponds to nepheline in which Na_2SO_4 groups are inserted into open spaces of the framework [10]. In view of the structural similarity between nosean and nepheline, the same detrimental effect by nosean is expected, namely damaging expansion. A volume expansion is most probably responsible for the unpredicted collapse of the wall lining, which was experienced by some incineration operators.

4 Conclusions

The refractory wear in the secondary combustion chamber of hazardous waste incinerators is caused by hot-corrosion, i.e. corrosion by alkali and sulphur vapours at moderate temperatures (700–1000 °C). Salt vapours and sulphur oxide infiltrate the brick via the open pore network. Subsequently, thenardite (Na_2SO_4) condenses inside the bricks, as soon as the temperature of the gas approaches the dew temperature. The interaction between thenardite and the refractory is related to the refractory material's silica content: the higher it is, the faster the corrosion proceeds. An important factor that impacts the corrosion rate is the mineralogical configuration. The chemical stability increases in the following order: amorphous silica (SiO_2) < cristobalite (SiO_2) < quartz (SiO_2) < andalusite (Al_2SiO_5) < mullite ($Al_6Si_2O_{13}$) < corundum (Al_2O_3). Alumina does not react with alkalis if the temperature remains below 1100 °C. For incineration operators it is important not to exceed this temperature. Otherwise, beta alumina ($11Al_2O_3 \cdot Na_2O$) may form, which causes catastrophic swelling [4].

A high alumina content is thus a suitable choice for the secondary combustion chamber. An ideal solution would be an utterly silica-free brick. Pure corundum bricks would withstand hot corrosion, but are cost-intensive.

An economical and adequate alternative are high-alumina refractories of at least 80 mass-% Al_2O_3 that contain as much alumina as possible in the bonding phase.

Moreover, this study has shown that neither the porosity nor a phosphate bonding influences significantly the resistance against corrosive vapours.

Thus, a high porosity does not accelerate the degradation, since even very low porosity materials are easily penetrated by the corrosive gases.

Acknowledgements

Extract of the Ph. D. thesis defended on April 2017 in Saint-Étienne/FR. This thesis was financed by BONY SA and the French National Association for Research and Technology (ANRT). The industrial test was conducted in a plant operated by SARPI-VEOLIA. The sample characterization was realized at MINES Saint-Étienne and CEMHTI-CNRS Orléans.

References

[1] Jacobson, N.S.; Smialek, J.L.; Fox, D.S.: Molten salt corrosion of ceramics. In: Corrosion of advanced ceramics: measurement and modelling proceedings of the NATO advanced research workshop on corrosion of advanced ceramics. Tübingen, Germany, 30. August–3. September 1993, Springer Netherlands 1994, 205–222

[2] Jacobson, N.S.: Corrosion of silicon-based ceramics in combustion environments. J. Amer. Ceram. Soc. **76** (1993) [1] 3–28

[3] Jacobson, N.S.: Sodium sulfate: deposition and dissolution of silica. Oxid. Met. **31** (1989) [1] 91–103

[4] Jacobson, N.S.; Lee, K.N.; Yoshio, T.: Corrosion of mullite by molten salts. J. Amer. Ceram. Soc. **79** (1996) [8] 2161–2167

[5] Opila, E.J.; Jacobson, N.S.: Oxidation and corrosion of ceramics. In: Ceramics science and technology, vol. 4: Applications, R. Riedel and I.-W. Chen, Eds. Weinheim 2013, 1–93

[6] Villalba Weinberg, A.; et al.: Corrosion of Al_2O_3–SiO_2 refractories by sodium and sulphur vapours: A case study on hazardous waste incinerators. Ceram. Int. **43** (2017) 5743–5750

[7] DIN EN 993-1, Method of test for dense shaped refractory products. Determination of bulk density, apparent porosity and true porosity, 1995

[8] De Crescente, M; Bornstein, N.: Formation and reactivity thermodynamics of sodium sulfate with gas turbine alloys. Corrosion **24** (1968) [5] 127–133

[9] Fryburg, G.C.; et al.: Formation of Na_2SO_4 and K_2SO_4 in flames doped with sulphur and alkali chlorides and carbonates. In: Symp. on High Temp. Metal Halide Chem., Atlanta 1977

[10] Gow, K.V.: Reaction of vaporized sodium sulfate with aluminous refractories. J. Amer. Ceram. Soc. **34** (1951) [11] 343–347

[11] Kohl, F.J.; et al.: Theoretical and experimental studies of the deposition of Na_2SO_4 from seeded combustion gases. J. Electrochem. Soc. **126** (1979) [6]1054–1061

[12] Lawson, M.G.; et al.: Hot corrosion of silica. J. Amer. Ceram. Soc. **73** (1990) [4] 989–995

[13] Nickel, K.G.; Quirmbach, P.; Pötschke, J.: Shreir's Corrosion, Chapter 1.26: High temperature corrosion of ceramics and refractory materials. Ed. T.J.A. Richardson, Amsterdam 2010, 668–690

[14] Zaitsev, A.; et al.: Thermodynamic properties and phase equilibria in the Na_2O–SiO_2 system. PCCP **1** (1999) [8] 1899–1907